ResearchArticle

Journal of Scientific Enquiry
Vol:3 (1) , Pages:19-23

Optimization of Mesh Density to Design Photonic Crystal Fiber employing Finite Element Method

S M Kamaruzzaman[1], Bibhatsu Kuiri[2], Ardhendu Sekhar Patra[2*]

[1]*College of Agricultural Engineering and Post Harvest Technology, Sikkim, India*
[2]*Sidho-Kanho-Birsha University, Purulia, West Bengal*

Received: 05.04.2023; accepted: 26.05.2023; published online: 30.06.2023

Abstract
In this work, a detailed investigation of photonic crystal fiber (PCF) with different mesh systems and degrees of freedom (DoF) is studied. The variation of numerical results is analysed using the finite element method (FEM). Fused silica as a cladding material was used to design the hollow core PCF and optimised for wavelength λ=1.55μm in the FEM analysis. Triangular mesh with growth rate (G_r) up to G_r =3.95 and maximum mesh element size (m_L) ranging from m_L=λ to m_L=14λ is used in the FEM study. The study shows field intensity deviation as high as ~100V/m and mode purity deviation up to 0.002%. This study puts light on the importance of meshing density and its effect on the deviation of the numerical outcome.

Keywords: Photonic Crystal Fiber, Finite Element Method, Mesh, Numerical Simulation

1. Introduction

The finite element method (FEM) is a well-known robust technique in the numerical study of different models, such as electromagnetic, mechanical, and structural models. The Finite Element Method (FEM) is a powerful numerical technique that has played a significant role in the advancement of engineering and applied sciences [1]. Furthermore, the integration of FEM with other computational techniques, such as optimisation algorithms and machine learning, has opened new horizons for the development of innovative solutions to complex engineering problems. Numerical simulation saves resources that otherwise could have been used in numerous experiments. Techniques such as finite difference approximations [1-3] and various weighted residual procedures [4] are used in different numerical studies. Coarse mesh settings will improve computational time but it will come at a cost of accuracy. So, there should be a balance between computational cost without compromising computational acceptable accuracy. Methods like FEM are handy to tackle problems and optimise the desired outcome before even testing in real life. The two kinds of meshing techniques used in filling the domain are triangular mesh [7] and quadrilateral mesh [8]. Solving FEM simulations requires meshing the model geometry. Among optical fibers, photonic crystal fiber (PCF) [9] has recently got much attention both for FEM-based study as well as possible candidates for advanced applications such as communication [10], sensing [11], and continuum generations [12], etc.

In this paper, we focus on two-dimensional simulation using Photonic Crystal Fiber (PCF) to understand the dependence of mesh on simulation results. Modelling is done in 2D geometry. Triangular mesh is used to fill the geometry. Analysis of mesh dependency on factors such as confinement loss, dispersion loss, mode purity and multimode effect of PCF is studied.

2. Theory and Design

The finite element method (FEM) is a modern, versatile tool that can give close approximate solutions to real experimental values in several fields of research. In our study, a PCF model in two-dimensional space is used as a reference model. The simulation is run for each wavelength λ. The mesh is prepared for the model with three important mesh parameters: Mesh growth (G_r), maximum mesh element size (m_L) and minimum element size (m_s). For each simulation and meshing of the model, these three parameters are needed to be set. The maximum and minimum possible element size of the mesh is limited by m_L and m_s. The model geometry is broken into a smaller domain called mesh domains formed by mesh elements, with a growth rate of mesh size G_r. Figure 1(a) shows the coarse mesh of sample geometry. Figure 1(b) shows the low-quality mesh responsible for the majority of deviation of results due to mesh. Figure 1(c) shows a representative image of the finer mesh. The mode analysis frequency is set to 193.1 THz. At the two media interfaces, when no surface current is present, the equation (1) and (2) is represented [13] as:

$$n_2 \times (E_1 - E_2) = 0 \quad (1)$$

$$n_2 \times (H_1 - H_2) = 0 \quad (2)$$

Here, E and H are the electric and magnetic fields for the two mediums. In the 2-Dimensional study, the electric field varies with the out-of-plane wave number k_z as

*email:ardhendu4u@yahoo.in

 DOI: https://doi.org/10.54280/jse.233104

Radius	μm	Area (air hole)	μm²	Material	R.I
r_1	6.90	a_1	23.42	Fused Silica	1.44
r_2	20.53	a_2	18.4	SF_2 doped	1.81
r_3	28.38			Air	1.00
r_4	37.83				

$$E_{(x,y,z)} = \bar{E}(x,y)exp(-ik_z z) \quad (3)$$

The wave equation (3) can be rearranged and written as the following[9]:

$$(\nabla - ik_z z) \times \left[\frac{1}{\mu_r}(\nabla - ik_2 z) \times E\right] - k_0^2 \varepsilon_{re} E = 0 \quad (4)$$

Where z is the out-of-the-plane (x-y plane) vector.

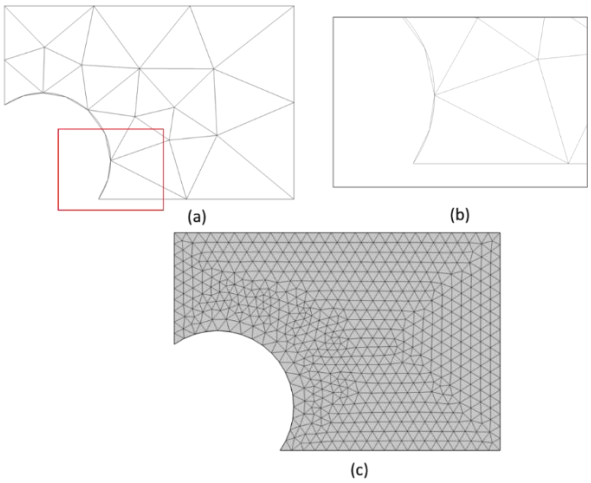

FIGURE 1(A) LOW-DENSITY MESH NEAR CURVED DOMAIN (B) MAGNIFIED VIEW SHOWING LOW-QUALITY MESH (C) DENSE MESH

The PCF design is shown in Figure 2.The inner core of radius r_1. The ring's inner and outer radii are r_2 and r_3, respectively. The final outer radius of the cladding is r_4. The outer air hole is composed of a circular hole of area a_1, and the inner ring is composed of modified rectangular holes of area a_2.

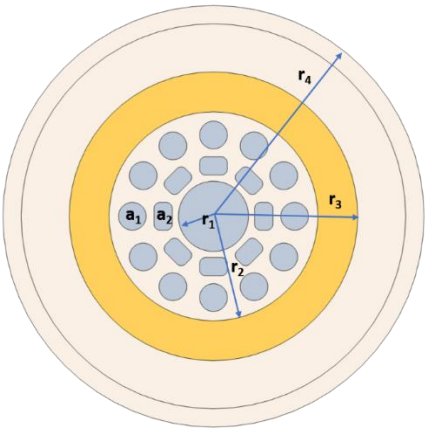

FIGURE 2 ARCHITECTURE OF PHOTONIC CRYSTAL FIBER FOR OPTIMISATION

The values are tabulated in Table 1 in micrometres (μm) and area as (μm²). The material used in the study includes fused silica, SF_2 doped silica and air.

Table 1 Geometry parameters for the model

Figure 2 shows two different types of mesh. We have designed the model using triangular mesh throughout the geometry domain of the PCF, as shown in Fig. 3(a). It contains 1012627 triangles, 940 edge elements, and 132 vertices. Fig 3(b) shows Quadrilateral meshing of the same PCF geometry. It contains 896 quadrilaterals, 902828 triangles, 1004 edge elements, 132 vertices. The study is set up for a frequency of 193.1 THz. All simulation is carried out using triangular mesh in this work. The outermost domain is set to a perfectly matched layer which is essentially used to handle reflected waves from the outer boundary.

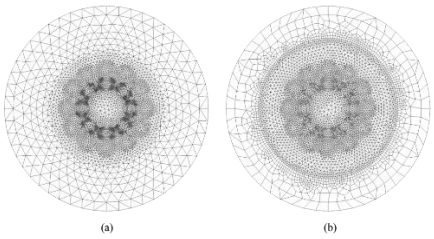

FIGURE 3 (A) PCF WITH TRIANGULAR MESH (B)PCF WITH QUADRILATERAL MESH

3. Results and Discussion

The numerical investigation is performed using the standard triangular mesh of the PCF geometry structure. The growth rate of the mesh, the maximum element size of the mesh, as well as the mode purity is analysed. Relative error calculation of mode purity is studied for different mesh growth rates.

Mesh growth rate analysis

The growth of adjacent mesh in filling up the model geometry is quantified by Mesh growth (G_r). Triangular mesh is used to fill up the domain for the FEM study. The field profile of a selected mode HE_{01}

is used as the reference model in the analysis. Figure 4 shows the dependence of mesh growth on the field intensity while keeping all other parameters unchanged. Results show at a fixed mesh size, the mesh growth density plays a major role in simulation results. The growth rate G_r=1.1 gives a field intensity of ~ 192 V/m, whereas, for G_r=3.95, the maximum field intensity is ~ 450 V/m, much higher than G_r=1.1. This increase is mainly attributed to the resulting coarse mesh near the boundary region between two different refractive indexes and curved geometry.

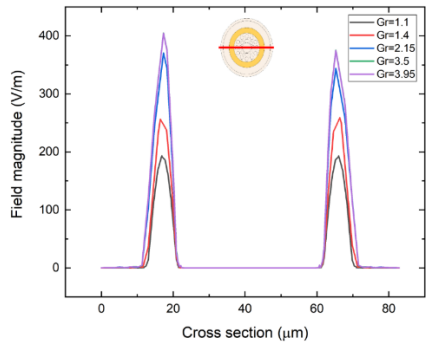

FIGURE 4 MESH GROWTH RATE VARIATION WITH THE FIELD MAGNITUDE THROUGH FIBER CROSS-SECTION PASSING THROUGH THE CENTRE

Maximum Mesh size analysis

We analysed the efficiency of the PCF for different sizes of mesh based on the field intensity studies. The maximum element size (m_L) of the mesh in Fig. 4 is varied with the excited wavelength λ. The maximum element size is varied from $m_{L=}$ λ to $m_{L=}$ 14λ. Minimum element size m_s and growth rate G_r are fixed at m_s = λ/12 and G_r=1.3, respectively. Figure 5 shows the variation of intensity magnitude due to m_L keeping all other parameters constant. The nature of the results is consistent. The data indicate that the magnitude of the maximum field intensity value (V/m) varies in the range of ~70 V/m in the studied model. Analysis shows the variation of peak intensity might deviate and should be taken care of while performing FEM-based electromagnetic simulations.

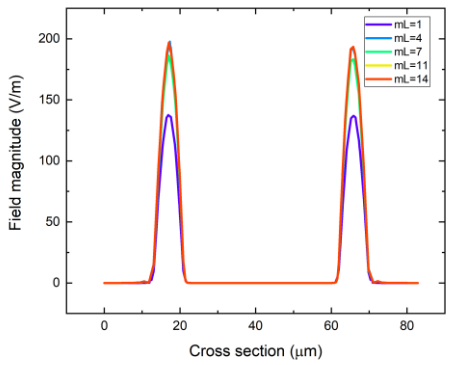

FIGURE 5 VARIATION OF FIELD INTENSITY DUE TO MAXIMUM MESH SIZE

The maximum intensity at different mesh dimensions is shown in the plot. Results indicate that even for identical simulation settings, the maximum intensity amplitude deviates to a relatively high value by setting different mL. Thus, these factors must be considered when working with electromagnetic-based simulations using the FEM technique.

Degree of freedom analysis

The quality of supported modes can be quantitively studied using the mode purity of the supported modes. The mode purity M_p is calculated using the following relation

$$M_p = \frac{I_{r1}}{I_{c1}} = \frac{\iint_{ring} |\vec{E}|^2 \, dxdy}{\iint_{cross\text{-}section} |\vec{E}|^2 \, dxdy} \quad (5)$$

Here I_{r1} and I_{c1} are the average mode field intensity in the PCF and the intensity of the whole area of the PCF, respectively, in the fiber. I_{r1} is the region where most of the intensity of all the OAM modes is supposed to be confined, which is the ring region. The calculation helps us to understand the quality of supported modes. Table 2 tabulates the G_r, mode purity, and degree of freedom (DoF) values for the given numerical study.

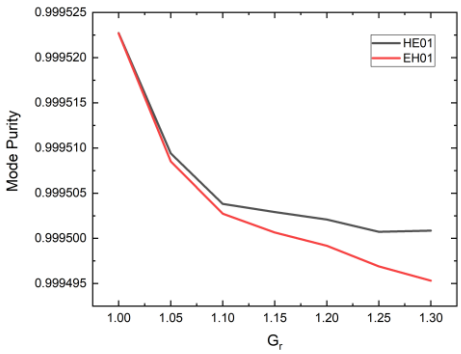

FIGURE 6 THE MODE PURITY WITH THE GROWTH RATE GR

TABLE 2: DEGREE OF FREEDOM SOLVED WITH THE GIVEN GROWTH RATE

G_r	Mode Purity (HE_{01})	Mode Purity (EH_{01})	DoF
1	0.999522716	0.999522688	653465
1.05	0.999509404	0.999508533	189113
1.1	0.999503807	0.999502733	141695
1.15	0.999502912	0.999500652	119365
1.2	0.999502091	0.99949919	107325
1.25	0.999500727	0.999496905	101963
1.3	0.999500851	0.999495313	96643

Error calculation due to mesh growth

The mesh growth is one of the fundamental parameters used in any FEM-based simulation, which is used in FEM-based PCF numerical simulations, but the effect of different mesh growth on the result is not intensively studied in literature as per our survey. Here we present the error calculation of mode purity with different growth rates. All other parameters are unchanged in this study. The G_r rate is checked from G_r=1 to G_r=1.3. The mode purity M_p at minimum growth rate G_r=1 is ~0.99952 from Table. 2. Relative Error is calculated using the value of M_p at G_r=1 as a reference.

$$M_p \text{ Error } \% = \frac{M_{p\,(G_r=1)} - M_{p\,(G_r=1.3)}}{M_{p\,(G_r=1)}} \quad (6)$$

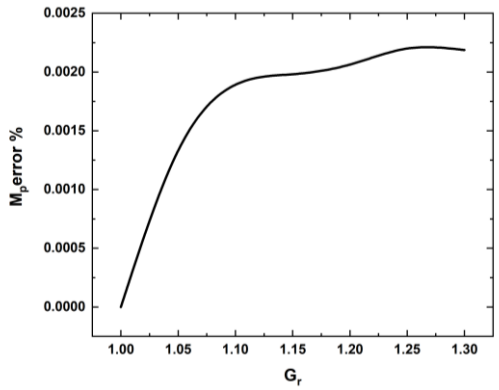

FIGURE 7 MODE PURITY ERROR CALCULATION TO GROWTH RATE FOR HE01

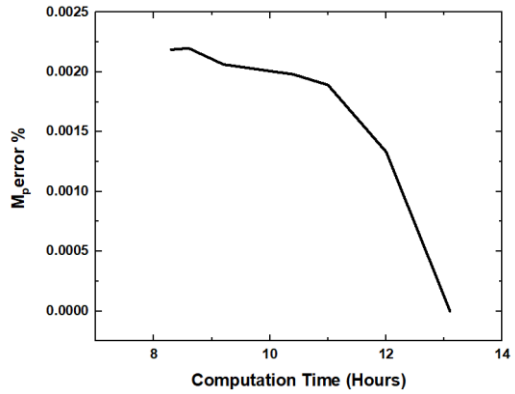

FIGURE 8 MODE PURITY ERROR CALCULATION TO COMPUTATIONAL TIME FOR HE01

Figure 7 shows the deviation in mode purity value at different growth rates. The total deviation is ~0.002% for our model and study settings. Figure 8 shows the relative error with computational time. The result accuracy depends on the mesh density as well as computational cost. A balance between optimum mesh density and computational resources are needed to be balanced for stable numerical simulation results. Coarse mesh will led to results at a cheaper computational cost but the results will come at an error bias, from our study Mode purity error came out to be +/- 0.002% with respect to the finest mesh used in the simulation. Even though this value looks small, in practicality, a PCF needs to be of finite long length where small changes through a distance can result in deviated results than theoretical prediction. Hence it is essential to consider the factors in the numerical designing process.

Conclusion

This study presents an intensive study of mesh dependence on PCF simulation based on FEM. The nature of the FEM study is consistent, but there is a significant deviation of peak intensity value at different mesh densities. The investigation shows deviation as high as ~100V/m for both G_r and m_L variation studies. The mesh element is varied from $m_L = \lambda$ to $m_L = 14\lambda$ for excited wavelength λ and growth rate G_r=1.1 to G_r=3.95. Mode purity of the supported mode of the PCF is calculated and yields a maximum relative error of ~ 0.002%. The study demonstrates the need for mesh optimisation, especially in developing sensors and sensitive optical instruments, as a small relative error may lead to a larger peak deviation. The study demonstrates the need to focus on mesh optimisation in FEM studies, particularly for photonic devices.

References

[1]. L.F. Richardson. The approximate arithmetical solution by finite differences of physical problems.Trans. Roy. Soc. (London), A210:307–357, 1910

[2]. R.V. Southwell. Relaxation Methods in Theoretical Physics. Clarendon Press, Oxford, 1st edition, 1946.

[3]. D.N. de G. Allen. Relaxation Methods. McGraw-Hill, London, 1955

[4]. B.A. Finlayson. The Method of Weighted Residuals and Variational Principles. Academic Press, NewYork, 1972.

[5]. A. Hrenikoff. Solution of problems in elasticity by the framework method. J. Appl. Mech.,ASME, A8:169–175, 1941.

[6]. R.V. Southwell. Stress calculation in frame works by the method of systematic relaxation of constraints, Part I & II. Proc. Roy. Soc. London (A), 151:56–95, 1935.

[7]. Jameson, Anthony, and D. Mavriplis. “Finite volume solution of the two-dimensional Euler equations on a regular triangular mesh.” AIAA journal 24.4 (1986): 611-618.

[8]. Blacker, Ted D., and Michael B. Stephenson. “Paving: A new approach to automated quadrilateral mesh generation.” International journal for numerical methods in engineering 32.4 (1991): 811-847.

[9]. Hoo, Yeuk L., Wei Jin, Chunzheng Shi, Hoi L. Ho, Dong N. Wang, and Shuang C. Ruan. “Design and modeling of a photonic crystal fiber gas sensor.” Applied Optics 42, no. 18 (2003): 3509-3515.

[10]. Zhang L, Zhang K, Peng J, Deng J, Yang Y, Ma J. Circular photonic crystal fiber

supporting 110 OAM modes. Optics Communications. 2018 Dec 15;429:189-93.

[11]. Chakma S, Khalek MA, Paul BK, Ahmed K, Hasan MR, Bahar AN. Gold-coated photonic crystal fiber biosensor based on surface plasmon resonance: design and analysis. Sensing and bio-sensing research. 2018 Apr 1;18:7-12.

[12]. Wang, Yimin, Yonghua Zhao, J. S. Nelson, Zhongping Chen, and Robert S. Windeler. "Ultrahigh-resolution optical coherence tomography by broadband continuum generation from a photonic W.K. Hayman, Meromorphic functions, The Clarendon Press, Oxford, 1964.

[13]. O.P. Juneja, G.P. Kapoor and S.K. Bajpai, On the (p,q)-order and lower (p,q)-order of an entire function, J.Reine Angew. Math., Vol. 282, No. 1(1976), pp. 53-67.

[14]. D.Sato, On the rate of growth of entire functions of fast growth, Bull. Amer. Math. Soc., Vol. 69, No. 1(1963), pp. 411-414.

[15]. M. N. Sheremeta, Connection between the growth of maximum of the modulus of an entire function and the moduli of the coefficients of its power series expansion, Izv. Vyssh. Uchebn. Zaved Mat., Vol. 2(1967), pp. 100-108 (in Russian).

[16]. S.K.Singh and G.P.Barker, Slowly changing functions and their applications, Indian Journal Of Mathematics, Vol. 19, No. 1(1977), pp. 1-6.

[17]. D.Somasundaram and R. Thamizharasi, A note on the entire functions of L-bounded index and L-type, Indian Journal of Pure and Applied Mathematics, Vol.19, No.3(1988), pp. 284-293.

[18]. G. Valiron, Lectures on the general theory of integral functions, Chelsa Publishing Company, New York (NY) USA, 1949.

[19]. L. Yang, Value distribution theory, Springer-Verlag, Berlin, 1993.